TOWARDS SUSTAINABLE STEELMAKING – EFFICIENT ENERGETIC UTILIZATION OF BLAST FURNACE GAS VIA MOLTEN CARBONATE FUEL CELLS *

Aline Lima da Silva[1]
Nestor Cezar Heck[2]

Abstract
Pressurized molten carbonate fuel cell (MCFC) hybrid system can be seen as an innovative and promising technology for efficient conversion of blast furnace gas into electricity. In this context, the present study provides a steady-state model for MCFC system based on anode and cathode gas recirculation concept, with blast furnace gas being used as a fuel. The developed code allows calculating, in an iterative and integrated way, heat and mass balance for the whole system, by modeling each module, namely, reformer, MCFC stack, afterburner, mixers, spliters, gas and steam turbines, and air compressor. Adiabatic reformer was modeled according to entropy maximization, allowing a more straightforward integration with MCFC anode. Firstly, the model is validated for MCFC architecture operating on natural gas, and satisfactory agreement was found, when compared with theoretical data available from recent literature; in this case, the proposed architecture yields an electrical efficiency of 67%. Then, the simulation is carried out for MCFC system operating on blast furnace gas, considering an average gas composition (5%H_2, 1%CH_4, 18%CO_2, 23%CO, 53%N_2) from a charcoal blast furnace of a non-integrated producer with capacity of 200 tonnes of pig iron per day. The whole process flowsheet diagram (PFD) is provided for a designed 3.5 MW AC MCFC system, yielding 60.6% net AC electrical efficiency. Such a high efficiency is achieved for pressurized system (7.5 atm), single cell voltage of 0.77V, at current density of 1370 A/m^2. This high value for electrical efficiency could boost distributed generation from blast furnace gas. In this way, we provide an estimate of power production for several non-integrated pig iron producers located in Minas Gerais State.
Keywords: Molten Carbonate Fuel Cell; Modelling; Blast Furnace Gas; Energetic Efficiency

[1] *PhD, Lecturer, Metallurgical and Materials Engineering, Federal University of Minas Gerais, Belo Horizonte, Minas Gerais, Brazil.*
[2] *PhD, Lecturer, MetallurgicalEngineering, Federal Universityof Rio Grande do Sul, Porto Alegre, Rio Grande do Sul, Brazill*

** Technical contribution to the39º Seminário de Balanços Energéticos Globais e Utilidades e 33º Encontro de Produtores e Consumidores de Gases Industriais, part of the ABM Week, October 2nd-4th, 2018, São Paulo, SP, Brazil.*

1 INTRODUCTION

Nowadays, there is a great effort to establish sustainable steelmaking in Minas Gerais State, focusing both on substantial reduction of greenhouse gases as well as on the implementation of innovative technologies able to increase energetic efficiency. The implantation of sustainable and efficient technologies and processes can bring a very positive impact from environmental, social and economical perspectives, as can be seen in detailed description of the *Sustainable Steelmaking Project*, coordinated by Brazilian Ministry of Environment and United Nations Development Program [1].

The development of the steel industry in Brazil is of utmost importance for the country's growth and becomes more than necessary [2]. In addition, it is worth pointing out the increasing interest around the world in blast furnace gas (BFG) use for energy purposes. As compared with coke oven gas, the caloric value of BFG is too low to be used alone as fuel because of its high concentrations of carbon dioxide and nitrogen. In this way, electricity generation from BFG alone can be a very challenge task when non-integrated pig iron producers are considered.

The State of Minas Gerais is Brazil's largest pig iron producer in non-integrated charcoal steelmills, with sixty-eight developments and one hundred and nine blast furnaces, totaling an installed capacity of more than nine million tons of pig iron per annum [3].

In order to boost distributed generation from BFG, it is necessary the adoption of very high efficiency technologies, with the potential to convert a low calorific gas into electricity. As a consequence, BFG energy use for electricity generation could become an attractive economic activity for the non-integrated producer, avoiding that a pollutant gas is simply wasted to atmosphere.

In this context, high efficiency molten carbonate fuel cells (MCFC) based systems could be considered as suitable devices for this purpose. Compared with the traditional power generation system, the efficiency of MCFC is far higher as it is not limited by the Carnot cycle, and waste heat from the high temperature exhaust gas can be recovered [4].

In the present study, a recently designed pressurized MCFC hybrid system is considered for evaluation of BFG conversion into electricity. This architecture was considered in this work, because of its very high net AC electrical efficiency of 69% reported for operation with natural gas as fuel [4].

The present study provides a steady-state model for MCFC system based on anode and cathode gas recirculation concept. The developed code allows calculating, in an iterative and integrated way, heat and mass balance for the whole system, by modeling each module, namely, reformer, MCFC stack, afterburner, mixers, spliters, gas and steam turbines, and air compressor. Firstly, the model is validated for MCFC architecture operating on natural gas. Then, the simulation is carried out for MCFC system operating on blast furnace gas, considering an average gas composition (5%H_2, 1%CH_4, 18%CO_2, 23%CO, 53%N_2) from a charcoal blast furnace of a non-integrated producer with capacity of 200 tonnes of pig iron per day. The whole process flowsheet diagram (PFD) and performance data are provided for the designed hybrid MCFC system. Finally, an estimate of power production for several non-integrated pig iron producers located in Minas Gerais State is provided.

2 METHODOLOGY

2.1 Pressurized MCFC hybrid power system description

Figure 1shows the proposed architecture for molten carbonate fuel cell hybrid power system. Each material stream was identified with a number, from #1 to #16, to facilitate the description of the system. Fuel (#1) is initially compressed until reaching the designed pressure ratio; then, compressed fuel (#2) is mixed with a portion of anode exhaust gas (#6), and the mixture (#3) is sent to reformer/shift reactor. When fuel is composed mainly of hydrocarbons, such as CH_4, steam reforming is the main chemical reaction, enabling the formation of $H_2$and CO, with monoxide carbon being converted into CO_2 through water-gas shift reaction ($CO+H_2O \rightarrow CO_2+H_2$). When fuel is the top gas from a charcoal blast furnace, some amount of CH_4 can be available and its reforming reaction occurs at some extent; however, in blast furnace gas, there is a great amount of CO that can be converted into H_2 through water-gas shift reaction. The approach of recycling anode exhaust (#6)is advantageous, because anode outlet gas is very rich in steam, besides allowing a thermal integration with reformer/shift reactor. The amount of gas from the anode to be routed to the reformer/shift reactor should be selected in such a way that carbon deposition free conditions are established inside reactor. The remaining part of the anode outlet gas(#7) is routed to the afterburner, where unreacted molecules of H_2, CO and CH_4 from anode outlet gas are burnt with residual O_2 from cathode exhaust (#11). A portion of afterburner outlet gas (#13) is mixed with compressed air (#9), and, this mixture (#10) is recycled to the cathode, where CO_2 electrochemically reacts with O_2, forming carbonate ion. The remaining portion of afterburner outlet gas (#14) is expanded in a turbine. The gas leaving turbine (#15) is still at high temperatureand can be used in a Heat Recovery Steam Generation (HRSG) unity, generating electricity in a steam turbine. Finally, exhaust gas (#16) is released to environment at 150ºC.

2.2. Mass and energy balance of the system

The steady-state model was implemented in Visual Basic. The algorithm flowchart is depicted in **Figure 2**. Basically, it consists of the following steps: (1) definition of operating parameters, (2) resolution of compressor models, (3) estimation of anode outlet composition and temperature for the main loop resolution; (4) estimation of afterburner outlet composition and temperature for the sub-loop resolution; (5) sequential resolution of mixer 1, reformer/shift reactor, chemical and electrochemical model of MCFC, mixer 2, thermal balance of stack, and afterburner model; (6) after main loop convergence, sequential resolution of Turbine 1 and HRSG (Heat Recovery Steam Generation) and ST (Steam Turbine) models are solved; (7) calculation of DC and AC system efficiencies. For a given set of operational parameters, the algorithm provides the whole process flowsheet diagram (PFD), that is, the composition, temperature and pressure for each material stream identified in the MCFC hybrid power system architecture. In order to solve the several models described in the algorithm flowchart, an optimization algorithm was employed. In the next section, a brief description of the component models is provided.

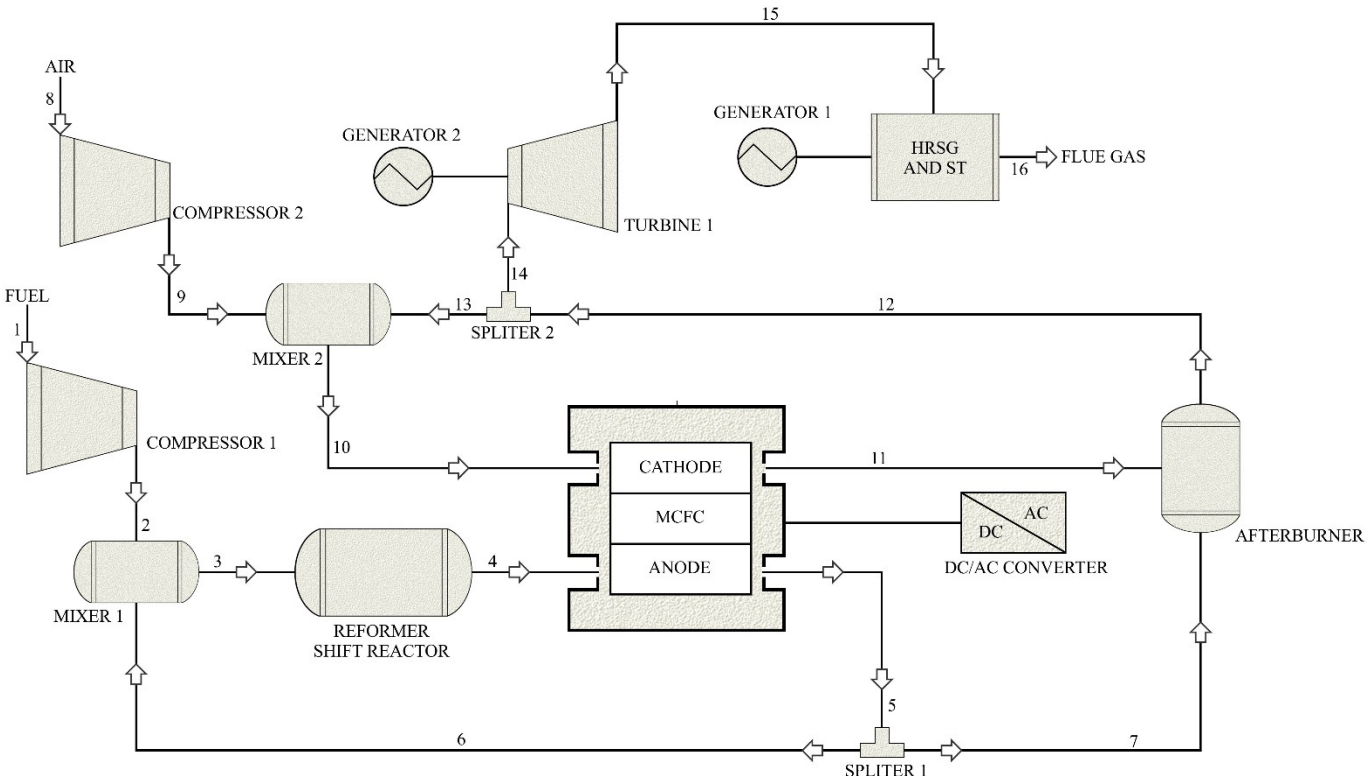

Figure 1. Molten carbonate fuel cell hybrid power system architecture.

2.3. Models Development

2.3.1. Adiabatic Reformer

The equilibrium composition and temperature of reformer outlet gas were simultaneously determined through entropy maximization. The optimization method seeks the maximum value for the system entropy (objective function, Eq. (1)) constrained by the elemental mass balance (Eq. (2)) and by isenthalpic condition (Eq. (3)) (restrictions).

$$S_{system} = \sum \dot{n}_i \bar{S}_i^0 - R \sum \dot{n}_i \ln(x_i P_{system}) \quad (1)$$

$$\sum_{i=1}^{N} \dot{n}_i \alpha_{ik} = b_k \quad (2)$$

$$\sum \dot{n}_{i,in} (\bar{H}_i)_{T=T_{inlet\_reformer}} - \sum \dot{n}_{i,out} (\bar{H}_i)_{T=T_{outlet\_reformer}} = 0 \quad (3)$$

In Eqs. (1)-(3), n_i and x_i correspond to molar flowrate (moles·s^{-1}) and molar fraction of species i, respectively; b_k is the number of moles of component k (C, H, O) in the system, and α_{ik} is the number of moles of component k in species i. In this study, $i \in \{H_2, H_2O, CH_4, CO, CO_2, N_2, C_{graphite}\}$. For validation with natural gas data, C_2H_6, C_3H_8, C_4H_{10} are also included in the species set.

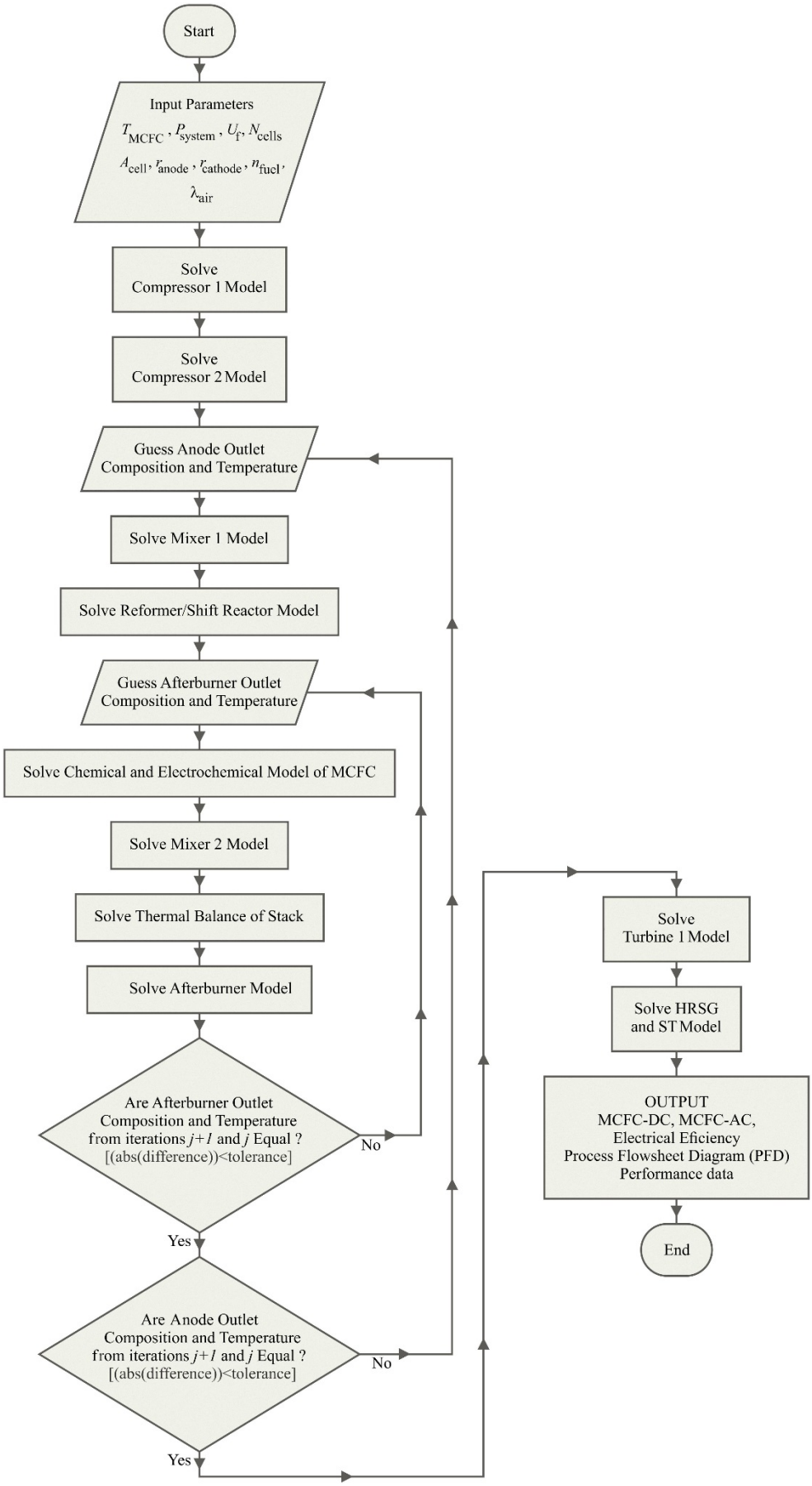

Figure 2. Solution algorithm of the MCFC hybrid power system model.

2.3.2. Molten Carbonate Fuel Cell

2.3.2.1. Electrochemical Model

The MCFC operating potential (V_{MCFC}) for a given current density i_{MCFC} is [5]:

$$V_{MCFC} = E_r - i_{MCFC} * (\eta_{act} + \eta_{conc} + \eta_{ohm}) \quad (4)$$

where E_r is the reversible open circuit voltage given by the Nernst equation, and η_{act}, η_{conc} and η_{ohm} correspond to activation, concentration and ohmic loss, respectively. The terms depicted in Eq. (4) are calculated as follows:

$$E_r = E_0 + \left[\frac{RT}{2F}\ln\left(\frac{P_{H_2,a} * P_{CO_2,c} * P_{O_2,c}^{0,5}}{P_{CO_2,a} * P_{H_2O,a}}\right)\right] \quad (5)$$

$$E_0 = 1.2723 - 2.7645 * 10^{-4} T \quad (6)$$

$$\eta_{act} = 2.27 * 10^{-9} * \exp\left(\frac{6435}{T}\right) * P_{H_2}^{-0.42} * P_{CO_2}^{-0.17} * P_{H_2O}^{-1.0} \quad (7)$$

$$\eta_{conc} = 7.505 * 10^{-10} * \exp\left(\frac{9298}{T}\right) * P_{O_2}^{-0.43} * P_{CO_2}^{-0.09} \quad (8)$$

$$\eta_{ohm} = 0.5 * 10^{-4} * \exp\left(3016 * \left(\frac{1}{T} - \frac{1}{923}\right)\right) \quad (9)$$

2.3.2.2. Chemical Model

For determination of the molar composition of the anode and cathode exhaust gas, the kinetics of three reactions occurring at the anode (methane internal reforming R1, water-gas shift R2, and hydrogen electrochemical oxidation R3), and the electrochemical reduction reaction at the cathode, R4, are considered:

$$CH_4 + H_2O \leftrightarrow CO + 3H_2 \quad (R1)$$

$$CO + H_2O \leftrightarrow CO_2 + H_2 \quad (R2)$$

$$2H_2 + 2CO_3^{2-} \rightarrow 2H_2O + 2CO_2 + 4e^- \quad (R3)$$

$$O_2 + 2CO_2 + 4e^- \rightarrow 2CO_3^{2-} \quad (R4)$$

Then, the system of equations to determine the number of moles of each species i(n_i) at the anode exhaust is given by:

$$n_i = n_i^0 + A_{cell} \sum v_{i\phi}\, r_\phi \quad (10)$$

where $v_{i\phi}$ is the stoichiometric coefficient of the species i in the reaction ϕ. The reaction rates (r_ϕ) for the above reactions are given by:

$$r_{R1=}k_{R1}P_a x_{CH_4} exp\left(\frac{-E_A}{RT}\right) \quad (11)$$

$$r_{R2} = k_{R2}P_a x_{CO}\left(1 - \frac{x_{CO_2}x_{H_2}/x_{CO}x_{H_2O}}{K_{R2}}\right) \quad (12)$$

$$r_{R3} = r_{R4} = \frac{i_{MCFC}}{2F} \quad (13)$$

2.3.2.3. Energy balance of MCFC stack

The energy balance of the stack is defined as follows:

$$\sum \dot{n}_{i,in}(\bar{H}_i)_{T=T_{inlet}} = \sum \dot{n}_{i,out}\ (\bar{H}_i)_{T=T_{outlet}} + P_{MCFC-DC} \quad (14)$$

where $P_{MCFC-DC}$ is DC power produced by MCFC stack, and it is given by:

$$P_{MCFC-DC} = N_{cells}\, A_{cell}\, i_{MCFC} V_{MCFC} \quad (15)$$

To keep the MCFC stack at a constant temperature, some cooling of the stack is required. Stack temperature can be kept constant when excess air is supplied to the cathode. The excess air ratio (λ_{air}) is defined as the ratio between the moles of oxygen supplied with air and moles of oxygen needed for electrochemical reaction.

2.3.3. Compressorand gas turbine

2.3.3.1. Compressor model

Based on perfect gas equations and polytropic transformations [6], the exhaust temperature can be determined by the following equation:

$$T_e = T_i\left(\frac{p_e}{p_i}\right)^{\frac{(\gamma-1)}{\gamma\eta_p}} \quad (16)$$

Where $\gamma = {}^{C_P}/_{C_V}$, and η_P is polytropic efficiency of the compressor.

Change in isentropic enthalpy is given by:

$$\Delta h_C = C_P T_i\left[\left(\frac{p_e}{p_i}\right)^{\frac{(\gamma-1)}{\gamma\eta_p}} - 1\right] \quad (17)$$

The compressor efficiency (η_C) is calculated by the following relationship:

$$\eta_C = \frac{\left(\frac{p_e}{p_i}\right)^{\frac{(\gamma-1)}{\gamma}} - 1}{\left(\frac{p_e}{p_i}\right)^{\frac{(\gamma-1)}{\gamma\eta_p}} - 1} \quad (18)$$

Compressor power consumption is calculated by:

$$P_C = \bar{C}_P \Delta T_C n_C \quad (19)$$

2.3.3.2. Turbine thermodynamic model

Turbine has been modeled in the same way as the compressor, following a polytropic expansion. The exhaust temperature:

$$T_e = T_i \left(\frac{p_e}{p_i}\right)^{\frac{(\gamma-1)\eta_p}{\gamma}} \quad (20)$$

Change in isentropic enthalpy:

$$\Delta h_T = C_P T_i \left[\left(\frac{p_e}{p_i}\right)^{\frac{(\gamma-1)\eta_p}{\gamma}} - 1\right] \quad (21)$$

Turbine efficiency (η_T):

$$\eta_T = \frac{1-\left(\frac{p_e}{p_i}\right)^{\frac{(\gamma-1)\eta_p}{\gamma}}}{1-\left(\frac{p_e}{p_i}\right)^{\frac{(\gamma-1)}{\gamma}}} \quad (22)$$

Turbine power generation is calculated by:

$$P_T = \bar{C}_P \Delta T_T n_T \quad (23)$$

Turbine should ideally produce more power than that required by the compression; mechanical power is assumed to be converted into electrical AC at 76.8% efficiency (96% gearbox) ×(80%mechanical to AC) [7]. It is assumed an efficiency of 95% for electric motor to drive centrifugal compressor.

2.3.4. Heat Recovery Steam Generator and Steam Turbine

A Rankine cycle with thermal efficiency of 26% is considered in the present study. In this cycle, liquid water at 38ºC and 9kPa is pumped until reaching 16MPa. Then, in a boiler, super-heated steam is generated at 15MPa and 600ºC. Pressurized steam is expanded in a turbine with 85% isentropic efficiency, and mechanical power is converted into electrical AC at 76.8% efficiency.

2.3.5. Afterburner

The equilibrium composition and temperature of afterburner outlet gas were determined through the entropy maximization, in a procedure similar to that of reformer. In this case, the selected species were: $\{H_2, H_2O, CH_4, CO, CO_2, O_2, N_2, NO, NO_2, N_2O\}$. One found that the only stable species were H_2O, CO_2, O_2 and N_2. NO_x species molar fraction was always lower than 10^{-5}.

3. RESULTS AND DISCUSSION

3.1. Validation with literature data for pressurized molten carbonate fuel cell hybrid system operating on natural gas

In the first part of this study, a system performance comparison is carried out, for validation purpose of the proposed steady-state model. Data from the present work are compared with those recently reported by Duan*et al*. [4]. **Table 1** shows the simulation conditions adopted, and **Table 2** depicts a comparison between power produced and system net AC efficiency. As one can see, relative error is below 3%, and good agreement is found. The efficiencies in the range of 67-69% for natural gas conversion are noteworthy; in fact, some fuel cell developers have reported efficiencies around 70 %LHV for natural gas pipelines applications in Connecticut.

Table 1. Simulation conditions

Atmosphericconditions	25ºC, 0.1MPa
Fuel mole composition	93.6%CH_4,4.9%C_2H_6, 0.4%C_3H_8, 0.2%C_4H_{10}, 0.9%CO
LHV offuel	49152.58kJ/kg
Fuelflow	3.85kg/s
Fuelutilizationratio	85%
Currentdensity	1500 A/m^2
Cathoderecycleratio	82.2%
Temperature	650ºC
DC/AC converter efficiency	92%
Air flow	130.46kg/s
Anoderecycleratio	68.5%

Table 2. Comparison between simulation results from this work and Duan et al. [4].

Output values	Thiswork	Duan et al.[4]	Relativeerror (%)
MCFC AC power, MW	107.73	106.23	1.4
System net power, MW	127.50	131.21	2.8
System net AC efficiency, %	67.34	69.34	2.9

3.2. Hybrid pressurized MCFC power system designed at net 3.5 MW AC

A hybrid pressurized MCFC power system was designed for a non-integrated charcoal blast furnace with capacity of 200 tonnes of pig iron per day. It is considered a production of 1500m^3 of gas per tonne of pig iron. However, it is assumed that 50% is available for electricity generation. The average gas composition considered for a charcoal blast furnace is: 5%H_2, 1%CH_4, 18%CO_2, 23%CO, 53%N_2[3].
The process flowsheet diagram (PFD) for the architecture depicted in **Figure 1** is shown in **Table 3** with each material stream given in terms of mass flowrate. **Table 4** shows the PFD given in terms of molar concentration (mol%).

Table 3. Process flowsheet diagram for hybrid MCFC system running on top gas from a charcoal blast furnace. Mass flowrate (kg·s^{-1}), temperature (K) and pressure (atm)are shown for each stream (#1 to #16, **Figure 1**).

Species	#1	#2	#3	#4	#5	#6	#7	#8	#9	#10	#11	#12	#13	#14	#15	#16
H_2O	0.00	0.00	0.35	0.36	0.44	0.35	0.09	0.00	0.00	0.42	0.42	0.51	0.42	0.09	0.09	0.09
CH_4	0.01	0.01	0.01	0.00	0.00	0.00	0.00	0.00	0.00	0.00	0.00	0.00	0.00	0.00	0.00	0.00
CO	0.46	0.46	0.53	0.57	0.09	0.07	0.02	0.00	0.00	0.00	0.00	0.00	0.00	0.00	0.00	0.00
CO_2	0.56	0.56	9.57	9.53	11.27	9.01	2.25	0.00	0.00	6.19	5.22	7.50	6.19	1.31	1.31	1.31
H_2	0.07	0.07	0.08	0.10	0.01	0.01	0.00	0.00	0.00	0.00	0.00	0.00	0.00	0.00	0.00	0.00
O_2	0.00	0.00	0.00	0.00	0.00	0.00	0.00	1.12	1.12	4.69	4.33	4.32	3.57	0.76	0.76	0.76
N_2	1.05	1.05	5.27	5.27	5.27	4.22	1.05	3.69	3.69	26.04	26.04	27.09	22.35	4.74	4.74	4.74
T(K)	298.0	658.7	891.4	878.6	923.0	923.0	923.0	298.0	582.2	919.9	965.9	966.4	966.4	966.4	662.7	423.0
P(atm)	1.00	7.58	7.57	7.56	7.50	7.50	7.50	1.00	7.56	7.55	7.50	7.43	7.43	7.43	1.02	1.00

Table 4. Process flowsheet diagram for hybrid MCFC turbine system running on top gas from a charcoal blast furnace. Molar concentration (mol%), temperature (K) and pressure (atm)are shown for each stream (#1 to #16, **Figure 1**)

Species	#1	#2	#3	#4	#5	#6	#7	#8	#9	#10	#11	#12	#13	#14	#15	#16
H_2O	0.0	0.00	4.33	4.39	5.14	5.14	5.14	0.00	0.00	1.89	1.94	2.18	2.18	2.18	2.18	2.18
CH_4	1.00	1.00	0.16	0.01	0.00	0.00	0.00	0.00	0.00	0.00	0.00	0.00	0.00	0.00	0.00	0.00
CO	23.00	23.00	4.20	4.55	0.66	0.66	0.66	0.00	0.00	0.00	0.00	0.00	0.00	0.00	0.00	0.00
CO_2	18.00	18.00	48.48	48.11	54.21	54.21	54.21	0.00	0.00	11.34	9.83	13.10	13.10	13.10	13.10	13.10
H_2	5.00	5.00	0.89	1.11	0.12	0.12	0.12	0.00	0.00	0.00	0.00	0.00	0.00	0.00	0.00	0.00
O_2	0.00	0.00	0.00	0.00	0.00	0.00	0.00	21.00	21.00	11.80	11.22	10.38	10.38	10.38	10.38	10.38
N_2	53.00	53.00	41.95	41.82	39.87	39.87	39.87	79.00	79.00	74.97	77.01	74.34	74.34	74.34	74.34	74.34
T(K)	298.0	658.7	891.4	878.6	923.0	923.0	923.0	298.0	582.2	919.9	965.9	966.4	966.4	966.4	662.7	423.0
P(atm)	1.00	7.58	7.57	7.56	7.5	7.5	7.5	1.00	7.56	7.55	7.5	7.43	7.43	7.43	1.02	1.00

Table 5 shows a summary of the main performance data for designed hybrid MCFC system.

Table 5. Inlet conditions and performance data for MCFC hybrid system designed at 3.5MW AC

SIMULATION CONDITIONS	CathodicRecirculation (%)	82.5
	AnodicRecirculation (%)	80
	MCFC temperature (K)	923
	System operatingpressure (atm)	7.5
	Fuelutilization (%)	85.5
	DC/AC converter efficiency(%)	92
	Numberofcells	3100
	Single cell active cell (m^2)	1
	Air excessratio	3.18
OUTPUT VALUES	Currentdensity (Am^{-2})	1369
	Single cellvoltage (V)	0.76
	MCFC DC power (MW)	3.25
	MCFC AC power (MW)	3.00
	Gas turbine power (MW)	0.81
	Steam turbine (MW)	0.48
	Fuel compressor consumption (MW)	0.77
	Net AC power (MW)	3.51
	Net AC electricalefficiency (%)	60.6

3.3. Electricity generation potential from charcoal blast furnaces located in Minas Gerais

Based on considerations and the results presented in **section 3.2**, one can estimate the electricity generation potential forseveral non-integrated pig iron producers located in Minas Gerais. Data for company, localization and pig iron production were obtained from Mallard [3]. **Table 6** shows that net AC power is in the range of 520kW to 24.3 MW. This result clearly shows that, amongst the existing fuel cells, molten carbonate fuel cells are more suitable.

Table 6. Electricity generation potential from blast furnace gas, considering non-integrated pig iron producers from Minas Gerais.

Non-integrated pig iron producers located in Minas Gerais				
Company	Localization	NumberofBlast Furnaces	Pig iron production (tonnes per day)	Estimated net AC power (MW)
AVG Siderurgia Ltda.	Sete Lagoas/MG	2	1000	17.38
Brasil Verde Agroindústrias Ltda.	Conceição do Pará/MG	1	220	3.82
Carmense Comercial Ltda.	Carmo da Mata/MG	1	56	0.97
Cia. Siderúrgica Pitangui	Pitangui/MG	3	930	16.16
Cisam Siderurgia Ltda.	Pará de Minas/MG	1	1400	24.33
Citygusa Siderurgia Ltda.	Pedro Leopoldo/MG	1	250	4.35
Cosimat - Siderúrgica Matozinhos Ltda.	Matozinhos/MG	2	700	12.17
Cossisa - Cia. Setelagoana de Siderurgia	Sete Lagoas/MG	3	730	12.69
Divigusa Indústria e Comércio Ltda.	Divinópolis/MG	3	360	6.26
Ferdil Produtos Metalúrgicos Ltda.	Divinópolis/MG	1	120	2.09
Ferdil Produtos Metalúrgicos Ltda.	São Gonçalo do Pará/MG	1	120	2.09
Fergubel - Ferro Gusa Bela Vista Ltda.	Matozinhos/MG	1	220	3.82
Fergubrás Ferro Gusa do Brasil Ltda.	Sete Lagoas/MG	2	550	9.56
Ferguminas Siderurgia Ltda.	Itaúna/MG	2	1000	17.38
Ferroeste Industrial Ltda.	Divinópolis/MG	1	200	3.48
Fundivale	Divinópolis/MG	1	220	3.82
Gerdau Aços Longos S.A	Contagem/MG	2	700	12.17
Gerdau Aços Longos S.A.	Sete Lagoas/MG	2	610	10.60
Hubner Siderurgia Unidade Minas Gerais Ltda.	São Gonçalo do Pará/MG	1	120	2.09
Insivi - Indústria Siderúrgica Viana Ltda.	Sete Lagoas/MG	4	1120	19.47
Ironbrás Indústria e Comércio S.A. - Usina I	Sete Lagoas/MG	1	400	6.95
Ironbrás Indústria e Comércio S.A. - Usina II	Sete Lagoas/MG	1	340	5.91
Itametal Siderurgia Ltda.	Itaúna/MG	1	170	2.95

Itasider - Usina Siderúrgica Itaminas S.A.	Sete Lagoas/MG	2	800	13.91
Itasider - Usina Siderúrgica Itaminas S.A.	Nova Serrana/MG	2	600	10.43
Mat-Prima Comércio de Metais Ltda.	Divinópolis/MG	2	230	4.00
Metalsete Siderurgia Ltda.	Sete Lagoas/MG	1	150	2.61
Metalsider Ltda.	Betim/MG	7	1260	21.90
MGS - Minas Gerais Siderurgia Ltda.	Sete Lagoas/MG	1	400	6.95
Minas Gusa Siderurgia Ltda.	Itaúna/MG	1	115	2.00
Nether Iron Siderurgia do Brasil S.A.	Bom Despacho/MG	1	120	2.09
Plantar Siderúrgica S.A.	Sete Lagoas/MG	2	680	11.82
Sama - Santa Marta Siderurgia Ltda.	Sete Lagoas/MG	1	200	3.48
Sicafe Produtos Siderúrgicos Ltda.	Sete Lagoas/MG	3	610	10.60
Siderbrás - Siderúrgica Brasileira Ltda.	Sete Lagoas/MG	2	300	5.21
Siderlagos Siderurgia Ltda.	Sete Lagoas/MG	1	270	4.69
Sidermin - Siderúrgica Mineira Ltda.	Sete Lagoas/MG	2	520	9.04
Siderpa - Siderúrgica Paulino Ltda.	Sete Lagoas/MG	2	610	10.60
Siderprata - Cia. Siderúrgica Lagoa da Prata	Lagoa da Prata/MG	1	200	3.48
Siderúrgica Álamo Ltda.	Divinópolis/MG	1	136	2.36
Siderúrgica Alterosa Ltda. - Unidade I	Pará de Minas/MG	2	500	8.69
Siderúrgica Alterosa Ltda. - Unidade II	Pará de Minas/MG	1	230	4.00
Siderúrgica Bandeirante Ltda.	Sete Lagoas/MG	2	300	5.21
Siderúrgica Barão de Mauá Ltda.	Sete Lagoas/MG	1	30	0.52
Siderúrgica Gafanhoto Ltda.	Nova Serrana/MG	1	200	3.48
Siderúrgica Gagé Ltda.	Conselheiro Lafaiete/MG	1	250	4.35
Siderúrgica Noroeste Ltda.	Sete Lagoas/MG	1	250	4.35
Siderúrgica Piratininga Ltda.	Itaguara/MG	1	150	2.61
Siderúrgica Santo Antônio Ltda.	Itaúna/MG	1	450	7.82
Siderúrgica São Luiz Ltda.	Divinópolis/MG	2	350	6.08
Siderúrgica São Sebastião do Itatiaiuçu	Itatiaiuçu/MG	1	250	4.35
Siderúrgica Trevo Ltda.	Alfredo Vasconcelos/ MG	2	400	6.95
Siderúrgica Trevo Ltda.	Curvelo/MG	2	400	6.95
Siderúrgica União Bondespachense Ltda.	Bom Despacho/MG	2	480	8.34
Siderúrgica Valinho S.A.	Divinópolis/MG	2	330	5.74
Simar - Siderúrgica Maravilhas Ltda.	Maravilhas/MG	1	130	2.26
Socoimex Siderurgia Ltda.	Itabira/MG	1	300	5.21

Susa - Siderúrgica União Ltda.	Divinópolis/MG	1	350	6.08
TCF - Triunfo Comércio de Ferro Ltda.	Divinópolis/MG	2	320	5.56
Tecnosider Siderurgia Ltda.	Prudente de Morais/MG	2	450	7.82
TMG Siderurgia Ltda.	Divinópolis/MG	1	140	2.43
Transtril Comércio e Exportação Ltda.	Carmo do Cajuru/MG	1	150	2.61
Transtril Comércio e Exportação Ltda.	Mateus Leme/MG	1	60	1.04
Unisider - União Siderúrgica Ltda.	Divinópolis/MG	1	190	3.30
Usisete - Usina Siderúrgica de Sete Lagoas	Sete Lagoas/MG	2	500	8.69
Usival - Usina Siderúrgica Valadares Ltda.	Governador Valadares/MG	1	150	2.61
VDL Siderurgia Ltda.	Itabirito/MG	1	280	4.87
Veredas Siderurgia Ltda.	Sete Lagoas/MG	2	500	8.69
Total power				466.3

4CONCLUSION

A mathematical model based on thermodynamics was developed to compute process flowsheet diagram (PFD) and carry out performance analysis of a pressurized molten carbonate fuel cell hybrid system for operation with blast furnace gas from non-integrated charcoal blast furnaces. The validation of proposed architecture was carried out for natural gas, and satisfactory agreement was found, with the hybrid system yielding a net AC electrical efficiency of 67%. A net 3.5MW AC MCFC hybrid system operating on blast furnace gas yielding 60.6% of electrical efficiency was designed from a thermodynamic viewpoint, and detailed PFD was provided. In future, it is believed that the proposed architecture can contribute to boost distributed generation from blast furnace gas, due to very high electrical efficiency. Design solution based on high anode and cathode recirculation ratios (around 80%) and pressurized system (7.5 atm) is preferable for maximizing efficiency. Finally, the electricity generation potential from charcoal blast furnaces located in Minas Gerais is provided, and the power size for distributed generation ranges from 520kW to 24.3MW, which is very suited for MCFC application.

Acknowledgments

Aline Lima da Silva would like to thank PRPq-UFMG for assistance to the research of newly appointed professors (ADRC-2016).

REFERENCES

1 Sustainable Steelmaking Project - Brazilian Ministry of Environment. Available from: http://www.mma.gov.br/governanca-ambiental/geoprocessamento/itemlist/category/220-clima-politica-nacional-sobre-mudanca-do-clima-siderurgia-sustentavel. Access data: 30 june 2018.

2 Chaves E. L. Gestão ambiental do gás do alto forno e avaliação dos sistemas de controle atmosféricos de siderúrgica, viabilizando um sistema de geração de energia. Dissertação de mestrado. 156p. Universidade Federal de Santa Catarina – Programa de Pós-Graduação em Engenharia Ambiental, Florianópolis, SC, 2013.

3 Malard A.A.M. Avaliação ambiental do setor de siderurgia não-integrada a carvão vegetal do Estado de Minas Gerais. Dissertação de Mestrado. 201p. Universidade Federal de Ouro Preto – Programa de Pós-Graduação em Engenharia Ambiental, Ouro Preto, 2009.

4 Duan L, Yue L., Feng T, Lu H, Bian J. Study on a novel pressurized MCFC hybrid system with CO2 capture. Energy. 2009; 737-750.

5 Ramandi MY, Dincer I. Thermodynamic performance analysis of a molten carbonate fuel cell at very high current densities. Journal of Power Sources.2011; 8509-8518.

6 Chinda P, Brault P. The hybrid solid oxide fuel cell (SOFC) and gas turbine (GT) systems steady state modeling. International Journal of Hydrogen Energy. 2012; 37:9237-9248.

7 Whyatt GA, Chick LA. Electrical Generation for More-Electric Aircraft using Solid Oxide Fuel Cells. Pacific Northwest National Laboratory, Richland, 2012.